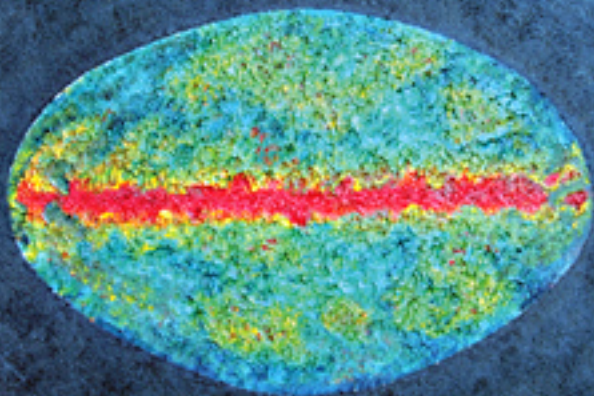


RUTH DURRER

THE
Cosmic Microwave
Background



CAMBRIDGE

CAMBRIDGE

www.cambridge.org/9780521847049

This page intentionally left blank

THE COSMIC MICROWAVE BACKGROUND

The cosmic microwave background (CMB) is the radiation left over from the big bang. Recent analysis of the fluctuations in this radiation has given us valuable insights into our Universe and its parameters.

This textbook examines the theory of CMB and its recent progress. It starts with a brief introduction to modern cosmology and its main successes, followed by a thorough derivation of cosmological perturbation theory. It then explores the generation of initial fluctuations by inflation. In the following chapters the Boltzmann equation, which governs the evolution of CMB anisotropies, and polarization are derived using the total angular momentum method. Cosmological parameter estimation is discussed in detail. The lensing of CMB fluctuations and spectral distortions are also treated.

The book is the first to contain a full derivation of the theory of CMB anisotropies and polarization. Ideal for graduate students and researchers in this field, the textbook includes end-of-chapter exercises, and solutions to selected exercises are provided.

Ruth Durrer is Professor of Theoretical Physics at the Université de Genève. Her research focuses on the cosmic microwave background, cosmic magnetic fields and braneworld cosmology.

THE COSMIC MICROWAVE BACKGROUND

RUTH DURRER

Université de Genève



CAMBRIDGE
UNIVERSITY PRESS

CAMBRIDGE UNIVERSITY PRESS

Cambridge, New York, Melbourne, Madrid, Cape Town, Singapore, São Paulo

Cambridge University Press

The Edinburgh Building, Cambridge CB2 8RU, UK

Published in the United States of America by Cambridge University Press, New York

www.cambridge.org

Information on this title: www.cambridge.org/9780521847049

© R. Durrer 2008

This publication is in copyright. Subject to statutory exception and to the provision of relevant collective licensing agreements, no reproduction of any part may take place without the written permission of Cambridge University Press.

First published in print format 2008

ISBN-13 978-0-511-42119-8 eBook (Adobe Reader)

ISBN-13 978-0-521-84704-9 hardback

Cambridge University Press has no responsibility for the persistence or accuracy of urls for external or third-party internet websites referred to in this publication, and does not guarantee that any content on such websites is, or will remain, accurate or appropriate.

To Martin, Florian, Melchior and Anna

Contents

	<i>Preface</i>	<i>page ix</i>
1	The homogeneous and isotropic universe	1
1.1	Homogeneity and isotropy	2
1.2	The background geometry of the Universe	3
1.3	Recombination and decoupling	14
1.4	Nucleosynthesis	27
1.5	Inflation	42
2	Perturbation theory	57
2.1	Introduction	57
2.2	Gauge-invariant perturbation variables	58
2.3	The perturbation equations	70
2.4	Simple examples	80
2.5	Light-like geodesics and CMB anisotropies	87
2.6	Power spectra	92
2.7	Final remarks	102
3	Initial conditions	105
3.1	Scalar field perturbations	106
3.2	Generation of perturbations during inflation	111
3.3	Mixture of dust and radiation revisited	121
4	CMB anisotropies	134
4.1	Introduction to kinetic theory	134
4.2	The Liouville equation in a perturbed FL universe	139
4.3	The energy–momentum tensor	143
4.4	The ultra-relativistic limit, the Liouville equation for massless particles	149
4.5	The Boltzmann equation	156
4.6	Silk damping	169
4.7	The full system of perturbation equations	171

5	CMB polarization and the total angular momentum approach	176
5.1	Polarization dependent Thomson scattering	177
5.2	Total angular momentum decomposition	183
5.3	The spectra	188
5.4	The small-scale limit and the physical meaning of \mathcal{E} and \mathcal{B}	194
5.5	The Boltzmann equation	199
6	Cosmological parameter estimation	210
6.1	Introduction	210
6.2	The physics of parameter dependence	211
6.3	Reionization	216
6.4	CMB data	217
6.5	Statistical methods	224
6.6	Degeneracies	245
6.7	Complementary observations	251
6.8	Sources	265
7	Lensing and the CMB	278
7.1	An introduction to lensing	278
7.2	The lensing power spectrum	282
7.3	Lensing of the CMB temperature anisotropies	283
7.4	Lensing of the CMB polarization	290
7.5	Non-Gaussianity	300
7.6	Other second-order effects	301
8	The CMB spectrum	304
8.1	Collisional processes in the CMB	304
8.2	A chemical potential	318
8.3	The Sunyaev–Zel’dovich effect	320
Appendix 1	Fundamental constants, units and relations	326
Appendix 2	General relativity	330
Appendix 3	Perturbations	335
Appendix 4	Special functions	340
Appendix 5	Entropy production and heat flux	357
Appendix 6	Mixtures	362
Appendix 7	Statistical utensils	364
Appendix 8	Approximation for the tensor C_ℓ spectrum	370
Appendix 9	Boltzmann equation in a universe with curvature	375
Appendix 10	The solutions of some exercises	384
	<i>References</i>	392
	<i>Index</i>	399

Preface

Cosmology, the quest concerning the Universe as a whole, has been a primary interest of human study since the beginnings of mankind. For a long time our ideas about the Universe were dominated by religious beliefs – tales of creation. Only since the advent of general relativity in 1915 have we had a scientific theory at hand that might be capable of describing the Universe. Soon after Einstein's first attempt of a static universe, Hubble and collaborators (Hubble, 1929) discovered that the observable Universe is expanding. This together with the discovery of the cosmic microwave background (CMB) by Penzias and Wilson (Nobel prize 1978) has established the theory of an expanding and cooling universe which started in a 'big bang'.

For a long time observations that have led to the determination of cosmological parameters, such as the rate of expansion, the so-called Hubble parameter, the mean matter density of the Universe, or its curvature, have been very sparse and we could only determine the order of magnitude of these parameters.

During the last decade this situation has changed significantly and cosmology has entered an era of precision measurements. This major breakthrough is to a large extent due to precise measurement and analysis of the CMB. In this book I develop the theory which is used to analyse and understand measurements of the CMB, especially of its anisotropies and polarization, but also its frequency spectrum. The Nobel prize was awarded to George Smoot and John Mather, in 2006, for the discovery of these anisotropies and for precise measurements of the CMB spectrum.

The book is directed mainly towards graduate students and researchers who want to obtain an overview of the main developments in CMB physics, and who want to understand the state-of-the-art techniques which are used to analyse CMB data. I believe that the theory of CMB physics is now sufficiently mature for a book on this topic to be useful. I shall not enter into any details concerning CMB experiments. This is by no means because I consider them less interesting, but rather that they

are still in full development and will hopefully make significant progress in the near future. Of course, my background is also that of a theoretical physicist and my main interest lies in the theoretical aspects of CMB physics. I hope, however, that this book will also be useful to CMB experimentalists who want to know what happens inside their cosmic parameter estimation routines.

It is assumed that the reader is familiar with undergraduate physics including the basics of general relativity, and has an elementary knowledge of quantum field theory and particle physics. The beauty of cosmology lies in the fact that it employs more or less all fields of physics starting with general relativity over thermodynamics and statistical physics to electrodynamics, quantum mechanics and particle physics. In this book I do not want to present an introduction to these topics as well since, first of all, there exist wonderful textbooks on all of them and second you have learned them in your undergraduate physics courses.

Before we start, let me sketch the content of the different chapters and give you a guide on how to read this book.

The first chapter is an overview of the homogeneous and isotropic universe. We present and discuss the Friedmann equations, recombination, nucleosynthesis and inflation. Readers familiar with cosmology may skip this chapter or just skim it.

In Chapter 2 we develop cosmological perturbation theory. This is the basics of CMB physics. The main reason why the CMB allows such an accurate determination of cosmological parameters lies in the fact that its anisotropies are small and can be determined within first-order perturbation theory. In Fourier space the linear perturbation equations become a series of ordinary linear differential equations, which can be solved numerically to high precision without any difficulty. We derive the perturbations of Einstein's equations and the energy-momentum conservation equations and solve them for simple but relevant cases. We also discuss the perturbation equation for light-like geodesics. This is sufficient to calculate the CMB anisotropies in the so-called instant recombination approximation. The main physical effects which are missed in such a treatment are Silk damping on small scales and polarization. We then introduce the CMB power spectrum and draw our first conclusions for its dependence on cosmological and primordial parameters. For example, we derive an approximate formula for the position of the acoustic peaks. An experimentalist mainly interested in parameter estimation may jump, after Chapter 2, directly to Chapter 6 and skip the more theoretical parts between.

The third chapter is devoted to the initial condition. There we explain how the unavoidable quantum fluctuations are amplified during an inflationary phase and lead to a nearly scale-invariant spectrum of scalar and tensor perturbations. We also discuss the initial conditions for mixed adiabatic and iso-curvature perturbations.

In Chapter 4 we derive the perturbed Boltzmann equation for CMB photons. After a brief introduction to relativistic kinetic theory, we first derive the Liouville

equation, i.e. the Boltzmann equation without a collision term. We also discuss the connection between the distribution function and the energy–momentum tensor. We then derive the collision term, i.e. the right-hand side of the Boltzmann equation, due to Thomson scattering of photons and electrons. In this first attempt we neglect the polarization dependence of Thomson scattering. The chapter ends with a list of the full system of perturbation equations for a Λ CDM universe.

In Chapter 5 we discuss polarization. Here we derive the total angular momentum method that is perfectly adapted to the problem of CMB anisotropies and polarization, taking into account its symmetry, which allows a decomposition into modes with fixed total angular momentum. The representation theory of the rotation group and the spin weighted spherical harmonics which are extensively used in this chapter are deferred to an appendix. We interpret some results using the flat sky approximation, which is valid on small angular scales.

Chapter 6 is devoted to parameter estimation. We first discuss the physical dependence of CMB anisotropies on cosmological parameters. After a section on CMB data we then treat in some detail statistical methods for CMB data analysis. We discuss especially the Fisher matrix and explain Markov chain Monte Carlo methods. We also address degeneracies, combinations of cosmological parameters on which CMB anisotropies do not, or only very weakly, depend. Because of these degeneracies, cosmological parameter estimation also makes use of other, non-CMB related, observations. We summarize them in a separate section. We finish the chapter with a discussion of ‘sources’, i.e. inhomogeneously distributed contributions to the energy–momentum tensor, such as topological defects, which may also contribute to the CMB anisotropies and thereby affect the estimated cosmological parameters.

In Chapter 7 we treat lensing of CMB anisotropies and polarization. This second-order effect is especially important on small scales but also has to be taken into account for $\ell \gtrsim 500$ if we want to achieve an accuracy of better than 0.5%. We first derive the deflection angle and the lensing power spectrum. Then we discuss lensing of CMB fluctuations and polarization in the flat sky approximation, which is sufficiently accurate for angular harmonics with $\ell \gtrsim 50$. We conclude the chapter with an overview on other second-order effects.

In the final chapter spectral distortions of the CMB are discussed. We first introduce the three relevant collision processes in a universe with photons and non-relativistic electrons: elastic Compton scattering, Bremsstrahlung and double Compton scattering. We derive the corresponding collision terms and Boltzmann equations. For elastic Compton scattering this leads us to the Kompaneets equation for which we present a detailed derivation. We introduce the timescales corresponding to these three collision processes and determine at which redshift a given process freezes – becomes slower than cosmic expansion. Finally, we discuss the

possible generation of a chemical potential in the CMB spectrum and the Sunyaev–Zel’dovich effect.

All chapters are complemented with some exercises at the end.

In the appendices we collect useful constants and formulae, information on special functions and some more technical derivations. The solutions to a selection of exercises are also given in an appendix.

This book has grown out of a graduate course on CMB anisotropies that I have given on several occasions. Thanks are due to the students of these courses, who have motivated me to write it up in the form of a textbook. I am also indebted to many collaborators and colleagues with whom I have discussed various aspects of the book and who have helped me to clarify many issues. Especially I want to mention Chiara Caprini, Martin Kunz, Toni Riotto, Uros Seljak and Norbert Straumann. I am also immensely grateful to students and colleagues who have read parts of the draft and helped me correct numerous typographical errors and other mistakes: Camille Bonvin, Jean-Pierre Eckmann, Alice Gasparini, Sandro Scodeller and others. Of course all the remaining mistakes are entirely my responsibility. Marcus Ruser and Martin Kunz have also helped me with some of the figures. I also wish to thank Susan Staggs who provided me with a most useful dataset of the CMB spectrum.

Ruth Durrer

1

The homogeneous and isotropic universe

Notation

In this book we denote the derivative with respect to physical time by a prime, and the derivative with respect to conformal time by a dot,

$$\tau = \text{physical (cosmic) time} \quad \frac{dX}{d\tau} \equiv X', \quad (1.1)$$

$$t = \text{conformal time} \quad \frac{dX}{dt} \equiv \dot{X}. \quad (1.2)$$

Spatial 3-vectors are denoted by a bold face symbol such as \mathbf{k} or \mathbf{x} whereas four-dimensional spacetime vectors are denoted as $x = (x^\mu)$.

We use the metric signature $(-, +, +, +)$ throughout the book.

The Fourier transform is defined by

$$f(\mathbf{k}) = \int d^3x f(\mathbf{x}) e^{i\mathbf{k}\cdot\mathbf{x}}, \quad (1.3)$$

so that

$$f(\mathbf{x}) = \frac{1}{(2\pi)^3} \int d^3k f(\mathbf{k}) e^{-i\mathbf{k}\cdot\mathbf{x}}. \quad (1.4)$$

We use the same letter for $f(\mathbf{x})$ and for its Fourier transform $f(\mathbf{k})$. The spectrum $P_f(k)$ of a statistically homogeneous and isotropic random variable f is given by

$$\langle f(\mathbf{k}) f^*(\mathbf{k}') \rangle = (2\pi)^3 \delta(\mathbf{k} - \mathbf{k}') P_f(k). \quad (1.5)$$

Since it is isotropic, $P_f(k)$ is a function only of the modulus $k = |\mathbf{k}|$. If f is Gaussian, the Dirac delta function implies that different \mathbf{k}' s are uncorrelated.

Throughout this book we use units where the speed of light, c , Planck's constant, \hbar and Boltzmann's constant, k_B are unity, $c = \hbar = k_B = 1$. Length and time therefore have the same units and energy, mass and momentum also have the same units, which are inverse to the unit of length. Temperature has the same units as energy.

We may use cm^{-1} to measure energy, mass, temperature, or eV^{-1} to measure distances or times. We shall use whatever unit is convenient to discuss a given problem. Conversion factors can be found in Appendix 1.

1.1 Homogeneity and isotropy

Modern cosmology is based on the hypothesis that our Universe is to a good approximation homogeneous and isotropic on sufficiently large scales. This relatively bold assumption is often called the ‘cosmological principle’. It is an extension of the Copernican principle stating that not only should our place in the solar system not be a special one, but also that the position of the Milky Way in the Universe should be in no way statistically distinguishable from the position of other galaxies. Furthermore, no direction should be distinguished. The Universe looks statistically the same in all directions. This, together with the hypothesis that the matter density and geometry of the Universe are smooth functions of the position, implies homogeneity and isotropy on sufficiently large scales. Isotropy around each point together with analyticity actually already implies homogeneity of the Universe.¹ A formal proof of this quite intuitive result can be found in [Straumann \(1974\)](#).

But which scale is ‘sufficiently large’? Certainly not the solar system or our galaxy. But also not the size of galaxy clusters. (In cosmology, distances are usually measured in Mpc (Megaparsec). $1 \text{ Mpc} = 3.2615 \times 10^6 \text{ light years} = 3.0856 \times 10^{24} \text{ cm}$ is a typical distance between galaxies, the distance between our neighbour Andromeda and the Milky Way is about 0.7 Mpc. These and other connections between frequently used units can be found in Appendix 1.)

It turns out that the scale at which the *galaxy distribution* becomes homogeneous is difficult to determine. From the analysis of the Sloan Digital Sky Survey (SDSS) it has been concluded that the irregularities in the galaxy density are still on the level of a few per cent on scales of $100 h^{-1} \text{ Mpc}$ ([Hogg et al., 2005](#)). Fortunately, we know that the *geometry* of the Universe shows only small deviations from the homogeneous and isotropic background, already on scales of a few Mpc. The geometry of the Universe can be tested with the peculiar motion of galaxies, with lensing, and in particular with the cosmic microwave background (CMB).

The small deviations from homogeneity and isotropy in the CMB are of uttermost importance since, most probably, they represent the ‘seeds’, which, via gravitational instability, have led to the formation of large-scale structure, galaxies and eventually solar systems with planets that support life in the Universe.

¹ If ‘analyticity’ is not assumed, the matter distribution could also be fractal and still statistically isotropic around each point. For a detailed elaboration of this idea and its comparison with observations see [Sylos Labini et al. \(1998\)](#).

Furthermore, we suppose that the initial fluctuations needed to trigger the process of gravitational instability stem from tiny quantum fluctuations that have been amplified during a period of inflationary expansion of the Universe. I consider this connection of the microscopic quantum world with the largest scales of the Universe to be of breathtaking philosophical beauty.

In this chapter we investigate the background Universe. We shall first discuss the geometry of a homogeneous and isotropic spacetime. Then we investigate two important events in the thermal history of the Universe. Finally, we study the paradigm of inflation. This chapter lays the basis for the following ones where we shall investigate *fluctuations* on the background, most of which can be treated in first-order perturbation theory.

1.2 The background geometry of the Universe

1.2.1 The Friedmann equations

In this section we assume a basic knowledge of general relativity. The notation and sign convention for the curvature tensor that we adopt are specified in Appendix A2.1.

Our Universe is described by a four-dimensional spacetime (\mathcal{M}, g) given by a pseudo-Riemannian manifold \mathcal{M} with metric g . A homogeneous and isotropic spacetime is one that admits a slicing into homogeneous and isotropic, i.e., maximally symmetric, 3-spaces. There is a preferred geodesic time coordinate τ , called ‘cosmic time’ such that the 3-spaces of constant time, $\Sigma_\tau = \{\mathbf{x} | (\tau, \mathbf{x}) \in \mathcal{M}\}$ are maximally symmetric spaces, hence spaces of constant curvature. The metric g is therefore of the form

$$ds^2 = g_{\mu\nu} dx^\mu dx^\nu = -d\tau^2 + a^2(\tau)\gamma_{ij} dx^i dx^j. \quad (1.6)$$

The function $a(\tau)$ is called the scale factor and γ_{ij} is the metric of a 3-space of constant curvature K . Depending on the sign of K this space is locally isometric to a 3-sphere ($K > 0$), a three-dimensional pseudo-sphere ($K < 0$) or flat, Euclidean space ($K = 0$). In later chapters of this book we shall mainly use ‘conformal time’ t defined by $a dt = d\tau$, so that

$$ds^2 = g_{\mu\nu} dx^\mu dx^\nu = a^2(t) (-dt^2 + \gamma_{ij} dx^i dx^j). \quad (1.7)$$

The geometry and physics of homogeneous and isotropic solutions to Einstein’s equations was first investigated mathematically in the early twenties by Friedmann (1922) and physically as a description of the observed expanding Universe in 1927

by Lemaître.² Later, Robertson (1936), Walker (1936) and others rediscovered the Friedmann metric and studied several additional aspects. However, since we consider the contributions by Friedmann and Lemaître to be far more fundamental than the subsequent work, we shall call a homogeneous and isotropic solution to Einstein's equations a 'Friedmann–Lemaître universe' (FL universe) in this book.

It is interesting to note that the Friedmann solution breaks Lorentz invariance. Friedmann universes are not invariant under boosts, there is a preferred cosmic time τ , the proper time of an observer who sees a spatially homogeneous and isotropic universe. Like so often in physics, the Lagrangian and therefore also the field equations of general relativity are invariant under Lorentz transformations, but a specific solution in general is not. In that sense we are back to Newton's vision of an absolute time. But on small scales, e.g. the scale of a laboratory, this violation of Lorentz symmetry is, of course, negligible.

The topology is not determined by the metric and hence by Einstein's equations. There are many compact spaces of negative or vanishing curvature (e.g. the torus), but there are no infinite spaces with positive curvature. A beautiful treatment of the fascinating, but difficult, subject of the topology of spaces with constant curvature and their classification is given in [Wolf \(1974\)](#). Its applications to cosmology are found in [Lachieze-Rey & Luminet \(1995\)](#).

Forms of the metric γ , which we shall often use are

$$\gamma_{ij} dx^i dx^j = \frac{\delta_{ij} dx^i dx^j}{(1 + \frac{1}{4}KR^2)^2}, \quad (1.8)$$

$$\gamma_{ij} dx^i dx^j = dr^2 + \chi^2(r) (d\theta^2 + \sin^2(\theta) d\varphi^2), \quad (1.9)$$

$$\gamma_{ij} dx^i dx^j = \frac{dR^2}{1 - KR^2} + R^2 (d\theta^2 + \sin^2(\theta) d\varphi^2), \quad (1.10)$$

where in Eq. (1.8)

$$\rho^2 = \sum_{i,j=1}^3 \delta_{ij} x^i x^j, \quad \text{and} \quad \delta_{ij} = \begin{cases} 1 & \text{if } i = j, \\ 0 & \text{else,} \end{cases} \quad (1.11)$$

and in Eq. (1.9)

$$\chi(r) = \begin{cases} r & \text{in the Euclidean case, } K = 0, \\ \frac{1}{\sqrt{K}} \sin(\sqrt{K}r) & \text{in the spherical case, } K > 0, \\ \frac{1}{\sqrt{|K|}} \sinh(\sqrt{|K|r}) & \text{in the hyperbolic case, } K < 0. \end{cases} \quad (1.12)$$

Often one normalizes the scale factor such that $K = \pm 1$ whenever $K \neq 0$. One has, however, to keep in mind that in this case r and K become dimensionless and the

² In the English translation of ([Lemaître, 1927](#)) from 1931 Lemaître's somewhat premature but pioneering arguments that the observed Universe is actually expanding have been omitted.

scale factor a has the dimension of length. If $K = 0$ we can normalize a arbitrarily. We shall usually normalize the scale factor such that $a_0 = 1$ and the curvature is not dimensionless. The coordinate transformations which relate these coordinates are determined in Ex. 1.1.

Due to the symmetry of spacetime, the energy–momentum tensor can only be of the form

$$(T_{\mu\nu}) = \begin{pmatrix} -\rho g_{00} & \mathbf{0} \\ \mathbf{0} & P g_{ij} \end{pmatrix}. \quad (1.13)$$

There is no additional assumption going into this ansatz, such as the matter content of the Universe being an ideal fluid. It is a simple consequence of homogeneity and isotropy and is also verified for scalar field matter, a viscous fluid or free-streaming particles in a FL universe. As usual, the energy density ρ and the pressure P are defined as the time- and space-like eigenvalues of (T_{ν}^{μ}) .

The Einstein tensor can be calculated from the definition (A2.12) and Eqs. (A2.31)–(A2.38),

$$G_{00} = 3 \left[\left(\frac{a'}{a} \right)^2 + \frac{K}{a^2} \right] \quad (\text{cosmic time}), \quad (1.14)$$

$$G_{ij} = - \left(2a''a + a'^2 + K \right) \gamma_{ij} \quad (\text{cosmic time}), \quad (1.15)$$

$$G_{00} = 3 \left[\left(\frac{\dot{a}}{a} \right)^2 + K \right] \quad (\text{conformal time}), \quad (1.16)$$

$$G_{ij} = - \left(2 \left(\frac{\dot{a}}{a} \right)^{\bullet} + \left(\frac{\dot{a}}{a} \right)^2 + K \right) \gamma_{ij} \quad (\text{conformal time}). \quad (1.17)$$

The Einstein equations relate the Einstein tensor to the energy–momentum content of the Universe via $G_{\mu\nu} = 8\pi G T_{\mu\nu} - g_{\mu\nu} \Lambda$. Here Λ is the so-called cosmological constant. In a FL universe the Einstein equations become

$$\left(\frac{a'}{a} \right)^2 + \frac{K}{a^2} = \frac{8\pi G}{3} \rho + \frac{\Lambda}{3} \quad (\text{cosmic time}), \quad (1.18)$$

$$2 \frac{a''}{a} + \frac{(a')^2}{a^2} + \frac{K}{a^2} = -8\pi G P + \Lambda \quad (\text{cosmic time}), \quad (1.19)$$

$$\left(\frac{\dot{a}}{a} \right)^2 + K = \frac{8\pi G}{3} a^2 \rho + \frac{a^2 \Lambda}{3} \quad (\text{conformal time}), \quad (1.20)$$

$$2 \left(\frac{\dot{a}}{a} \right)^{\bullet} + \left(\frac{\dot{a}}{a} \right)^2 + K = -8\pi G a^2 P + a^2 \Lambda \quad (\text{conformal time}). \quad (1.21)$$

Energy ‘conservation’, $T^{\mu\nu}_{;\mu} = 0$ yields

$$\dot{\rho} = -3(\rho + P) \left(\frac{\dot{a}}{a} \right) \quad \text{or, equivalently} \quad \rho' = -3(\rho + P) \left(\frac{a'}{a} \right). \quad (1.22)$$

This equation can also be obtained by differentiating Eq. (1.18) or (1.20) and inserting (1.19) or (1.21); it is a consequence of the contracted Bianchi identities (see Appendix A2.1). Eqs. (1.18)–(1.21) are the Friedmann equations. The quantity

$$H(\tau) \equiv \frac{a'}{a} = \frac{\dot{a}}{a^2} \equiv \mathcal{H}a^{-1}, \quad (1.23)$$

is called the Hubble rate or the Hubble parameter, where \mathcal{H} is the comoving Hubble parameter. At present, the Universe is expanding, so that $H_0 > 0$. We parametrize it by

$$H_0 = 100 h \text{ km s}^{-1} \text{ Mpc}^{-1} \simeq 3.241 \times 10^{-18} h \text{ s}^{-1} \simeq 1.081 \times 10^{-28} h \text{ cm}^{-1}.$$

Observations show (Freedman *et al.*, 2001) that $h \simeq 0.72 \pm 0.1$. Eq. (1.22) is easily solved in the case $w = P/\rho = \text{constant}$. Then one finds

$$\rho = \rho_0 (a_0/a)^{3(1+w)}, \quad (1.24)$$

where ρ_0 and a_0 denote the value of the energy density and the scale factor at present time, τ_0 . In this book cosmological quantities indexed by a ‘0’ are evaluated today, $X_0 = X(\tau_0)$. For non-relativistic matter, $P_m = 0$, we therefore have $\rho_m \propto a^{-3}$ while for radiation (or any kind of massless particles) $P_r = \rho_r/3$ and hence $\rho_r \propto a^{-4}$. A cosmological constant corresponds to $P_\Lambda = -\rho_\Lambda$ and we obtain, as expected $\rho_\Lambda = \text{constant}$. If the curvature K can be neglected and the energy density is dominated by one component with $w = \text{constant}$, inserting Eq. (1.24) into the Friedmann equations yields the solutions

$$a \propto \tau^{2/3(1+w)} \propto t^{2/(1+3w)} \quad w = \text{constant} \neq -1, \quad (1.25)$$

$$a \propto \tau^{2/3} \propto t^2 \quad w = 0, \quad (\text{dust}), \quad (1.26)$$

$$a \propto \tau^{1/2} \propto t \quad w = 1/3, \quad (\text{radiation}), \quad (1.27)$$

$$a \propto \exp(H\tau) \propto 1/|t| \quad w = -1, \quad (\text{cosmol. const.}). \quad (1.28)$$

It is interesting to note that if $w < -1$, so-called ‘phantom matter’, we have to choose $\tau < 0$ to obtain an expanding universe and the scale factor diverges in finite time, at $\tau = 0$. This is the so-called ‘big rip’. Phantom matter has many problems but it is discussed in connection with the supernova type 1a (SN1a) data, which are compatible with an equation of state with $w < -1$ or with an ordinary cosmological constant (Caldwell *et al.*, 2003). For $w < -\frac{1}{3}$ the time coordinate t has to be chosen as negative for the Universe to expand and spacetime cannot be

continued beyond $t = 0$. But $t = 0$ corresponds to a cosmic time, the proper time of a static observer, $\tau = \infty$; this is not a singularity. (The geodesics can be continued until affine parameter ∞ .)

We also introduce the adiabatic sound speed c_s determined by

$$c_s^2 = \frac{P'}{\rho'} = \frac{\dot{P}}{\dot{\rho}}. \quad (1.29)$$

From this definition and Eq. (1.22) it is easy to see that

$$\dot{w} = 3\mathcal{H}(1+w)(w - c_s^2). \quad (1.30)$$

Hence $w = \text{constant}$ if and only if $w = c_s^2$ or $w = -1$. Note that already in a simple mixture of matter and radiation $w \neq c_s^2 \neq \text{constant}$ (see Ex. 1.3).

Eq. (1.18) implies that for a critical value of the energy density given by

$$\rho(\tau) = \rho_c(\tau) = \frac{3H^2}{8\pi G} \quad (1.31)$$

the curvature and the cosmological constant vanish. The value ρ_c is called the critical density. The ratio $\Omega_X = \rho_X/\rho_c$ is the ‘density parameter’ of the component X . It indicates the fraction that the component X contributes to the expansion of the Universe. We shall make use especially of

$$\Omega_r \equiv \Omega_r(\tau_0) = \frac{\rho_r(\tau_0)}{\rho_c(\tau_0)}, \quad (1.32)$$

$$\Omega_m \equiv \Omega_m(\tau_0) = \frac{\rho_m(\tau_0)}{\rho_c(\tau_0)}, \quad (1.33)$$

$$\Omega_K \equiv \Omega_K(\tau_0) = \frac{-K}{a_0^2 H_0^2}, \quad (1.34)$$

$$\Omega_\Lambda \equiv \Omega_\Lambda(\tau_0) = \frac{\Lambda}{3H_0^2}. \quad (1.35)$$

1.2.2 The ‘big bang’ and ‘big crunch’ singularities

We can absorb the cosmological constant into the energy density and pressure by redefining

$$\rho_{\text{eff}} = \rho + \frac{\Lambda}{8\pi G}, \quad P_{\text{eff}} = P - \frac{\Lambda}{8\pi G}.$$

Since Λ is a constant and $\rho_{\text{eff}} + P_{\text{eff}} = \rho + P$, the conservation equation (1.22) still holds. A first interesting consequence of the Friedmann equations is obtained

when subtracting Eq. (1.18) from (1.19). This yields

$$\frac{a''}{a} = -\frac{4\pi G}{3}(\rho_{\text{eff}} + 3P_{\text{eff}}). \quad (1.36)$$

Hence if $\rho_{\text{eff}} + 3P_{\text{eff}} > 0$, the Universe is decelerating. Furthermore, Eqs. (1.22) and (1.36) then imply that in an expanding and decelerating universe

$$\frac{\rho'_{\text{eff}}}{\rho_{\text{eff}}} < -2\frac{a'}{a},$$

so that ρ decays faster than $1/a^2$. If the curvature is positive, $K > 0$, this implies that at some time in the future, τ_{max} , the density has dropped down to the value of the curvature term, $K/a^2(\tau_{\text{max}}) = 8\pi G\rho_{\text{eff}}(\tau_{\text{max}})$. Then the Universe stops expanding and recollapses. Furthermore, this is independent of curvature, as a' decreases the curve $a(\tau)$ is concave and thus cuts the $a = 0$ line at some finite time in the past. This moment of time is called the ‘big bang’. The spatial metric vanishes at this value of τ , which we usually choose to be $\tau = 0$; and spacetime cannot be continued to earlier times. This is not a coordinate singularity. From the Ricci tensor given in Eqs. (A2.31) and (A2.32) one obtains the Riemann scalar

$$R = 6 \left[\frac{a''}{a} + \left(\frac{a'}{a} \right)^2 + \frac{K}{a^2} \right],$$

which also diverges if $a \rightarrow 0$. Also the energy density, which grows faster than $1/a^2$ as $a \rightarrow 0$ diverges at the big bang.

If the curvature K is positive, the Universe contracts after $\tau = \tau_{\text{max}}$ and, since the graph $a(\tau)$ is convex, reaches $a = 0$ at some finite time τ_c , the time of the ‘big crunch’. The big crunch is also a physical singularity beyond which spacetime cannot be continued.

It is important to note that this behaviour of the scale factor can only be implied if the so-called ‘strong energy condition’ holds, $\rho_{\text{eff}} + 3P_{\text{eff}} > 0$. This is illustrated in Fig. 1.1.

1.2.3 Cosmological distance measures

It is notoriously difficult to measure distances in the Universe. The position of an object in the sky gives us its angular coordinates, but how far away is the object from us? This problem has plagued cosmology for centuries. It was only Hubble, who discovered around 1915–1920 that the ‘spiral nebulae’ are actually not situated inside our own galaxy but much further away. This then led to the discovery of the expansion of the Universe.

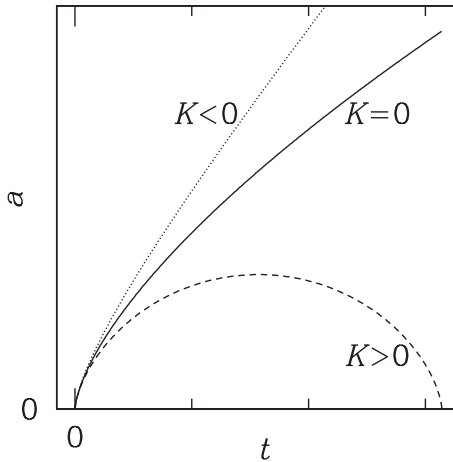


Fig. 1.1. The kinematics of the scale factor in a Friedmann–Lemaître universe which satisfies the strong energy condition, $\rho_{\text{eff}} + 3P_{\text{eff}} > 0$.

For cosmologically distant objects, a third coordinate, which is nowadays relatively easy to obtain, is the redshift z experienced by the photons emitted from the object. A given spectral line with intrinsic wavelength λ is redshifted due to the expansion of the Universe. If it is emitted at some time τ , it reaches us today with wavelength $\lambda_0 = \lambda a_0/a(\tau) = (1+z)\lambda$. This leads to the definition of the cosmic redshift

$$z(\tau) + 1 = \frac{a_0}{a(\tau)}. \quad (1.37)$$

On the other hand, an object at physical distance $d = a_0 r$ away from us, at redshift $z \ll 1$, recedes with speed $v = H_0 d$. To the lowest order in z , we have $\tau_0 - \tau \approx d$ and $a_0 \approx a(\tau) + a'(\tau_0 - \tau)$, so that

$$1 + z \approx 1 + \frac{a'}{a}(\tau_0 - \tau) \approx 1 + H_0 d.$$

For objects that are sufficiently close, $z \ll 1$ we therefore have $v \approx z$ and hence $H_0 = v/d$. This is the method usually applied to measure the Hubble constant.

There are different ways to measure distances in cosmology all of which give the same result in a Minkowski universe but differ in an expanding universe. They are, however, simply related as we shall see.

One possibility is to define the distance D_A to a certain object of given physical size Δ seen at redshift z_1 such that the angle subtended by the object is given by

$$\vartheta = \Delta/D_A, \quad D_A = \Delta/\vartheta. \quad (1.38)$$

This is the angular diameter distance, see Fig. 1.2.

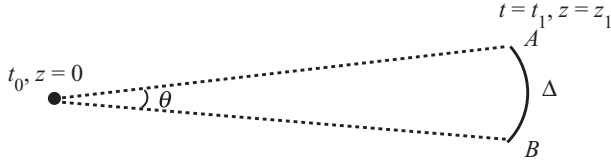


Fig. 1.2. The two ends of the object emit a flash simultaneously from A and B at z_1 which reaches us today. The angular diameter distance to A (or B) is defined by $D_A = \Delta/\vartheta$.

We now derive the expression

$$D_A(z) = \frac{1}{\sqrt{|\Omega_K|}H_0(1+z)} \chi \left(\sqrt{|\Omega_K|}H_0 \int_0^z \frac{dz'}{H(z')} \right), \quad (1.39)$$

for the angular diameter distance to redshift z . In a given cosmological model, this allows us to express the angular diameter distance for a given redshift as a function of the cosmological parameters.

To derive Eq. (1.39) we use the coordinates introduced in Eq. (1.9). Without loss of generality we set $r = 0$ at our position. We consider an object of physical size Δ at redshift z_1 simultaneously emitting a flash at both of its ends A and B . Hence $r = r_1 = t_0 - t_1$ at the position of the flashes, A and B at redshift z_1 . If Δ denotes the physical arc length between A and B we have $\Delta = a(t_1)\chi(r_1)\vartheta = a(t_1)\chi(t_0 - t_1)\vartheta$, i.e.,

$$\vartheta = \frac{\Delta}{a(t_1)\chi(t_0 - t_1)}. \quad (1.40)$$

According to Eq. (1.38) the angular diameter distance to t_1 or z_1 is therefore given by

$$a(t_1)\chi(t_0 - t_1) \equiv D_A(z_1). \quad (1.41)$$

To obtain an expression for $D_A(z)$ in terms of the cosmic density parameters and the redshift, we have to calculate $(t_0 - t_1)(z_1)$.

Note that in the case $K = 0$ we can normalize the scale factor a as we want, and it is convenient to choose $a_0 = 1$, so that comoving scales become physical scales today. However, for $K \neq 0$, we have already normalized a such that $K = \pm 1$ and $\chi(r) = \sin r$ or $\sinh r$. In this case, we have no normalization constant left and a_0 has the dimension of a length. The present spatial curvature of the Universe then is $\pm 1/a_0^2$.

The Friedmann equation Eq. (1.20) reads

$$\dot{a}^2 = \frac{8\pi G}{3}a^4\rho + \frac{1}{3}\Lambda a^4 - K a^2, \quad (1.42)$$

where $\dot{a} = da/dt$. To be specific, we assume that ρ is a combination of dust, cold, non-relativistic ‘matter’ of $P_m = 0$ and radiation of $P_r = \rho_r/3$.

Since $\rho_r \propto a^{-4}$ and $\rho_m \propto a^{-3}$, we can express the terms on the r.h.s. of (1.42) as

$$\frac{8\pi G}{3} a^4 \rho = H_0^2 (a_0^4 \Omega_r + \Omega_m a a_0^3), \quad (1.43)$$

$$\frac{1}{3} \Lambda a^4 = H_0^2 \Omega_\Lambda a^4, \quad (1.44)$$

$$-K a^2 = H_0^2 \Omega_K a^2 a_0^2. \quad (1.45)$$

The Friedmann equation then implies

$$\frac{da}{dt} = H_0 a_0^2 \left(\Omega_r + \frac{a}{a_0} \Omega_m + \frac{a^4}{a_0^4} \Omega_\Lambda + \frac{a^2}{a_0^2} \Omega_K \right)^{1/2}, \quad (1.46)$$

so that

$$t_0 - t_1 = \frac{1}{H_0 a_0} \int_0^{z_1} \frac{dz}{[\Omega_r(z+1)^4 + \Omega_m(z+1)^3 + \Omega_\Lambda + \Omega_K(z+1)^2]^{1/2}}. \quad (1.47)$$

Here we have used $z+1 = a_0/a$ so that $da = -dz a_0/(1+z)^2$.

In principle, we could of course also add other matter components like, e.g. ‘quintessence’ (Caldwell *et al.*, 1998), which would lead to a somewhat different form of the integral (1.47), but for definiteness, we remain with matter, radiation and a cosmological constant.

From $-K/H_0^2 a_0^2 = \Omega_K$ we obtain $H_0 a_0 = 1/\sqrt{|\Omega_K|}$ for $\Omega_K \neq 0$. The expression for the angular diameter distance thus becomes

$$D_A(z) = \begin{cases} \frac{1}{\sqrt{|\Omega_K|} H_0 (z+1)} \chi \left(\sqrt{|\Omega_K|} \int_0^z \frac{dz'}{[\Omega_r(z'+1)^4 + \Omega_m(z'+1)^3 + \Omega_\Lambda + \Omega_K(z'+1)^2]^{1/2}} \right) & \text{if } K \neq 0 \\ \frac{1}{H_0(z+1)} \int_0^z \frac{dz'}{[\Omega_r(z'+1)^4 + \Omega_m(z'+1)^3 + \Omega_\Lambda]^{1/2}} & \text{if } K = 0. \end{cases} \quad (1.48)$$

Using the Friedmann equation, this formula can also be written in the more general form of Eq. (1.39).

In general, the above integral has to be solved numerically. It determines the angle $\vartheta(\Delta, z) = \Delta/D_A(z)$ under which an object of size Δ placed at redshift z is seen (see Figs. 1.3 and 1.4).

If we are able to measure the redshifts and the angular extensions of a certain class of objects at different redshifts, of which we know the intrinsic size Δ , comparing

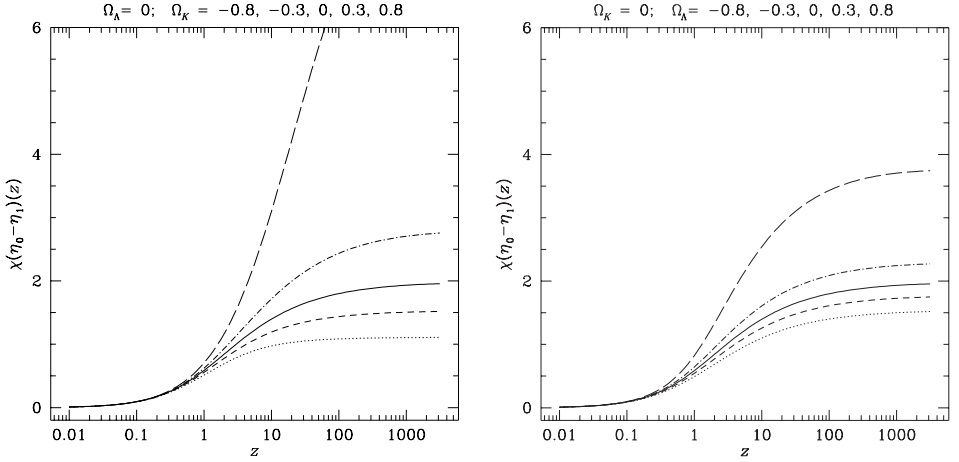


Fig. 1.3. The function $\chi(t_0 - t_1)$ as a function of the redshift z for different values of the cosmological parameters Ω_K (left, with $\Omega_\Lambda = 0$) and Ω_Λ (right, with $\Omega_K = 0$), namely -0.8 (dotted), -0.3 (short-dashed), 0 (solid), 0.3 (dot-dashed), 0.8 (long-dashed).

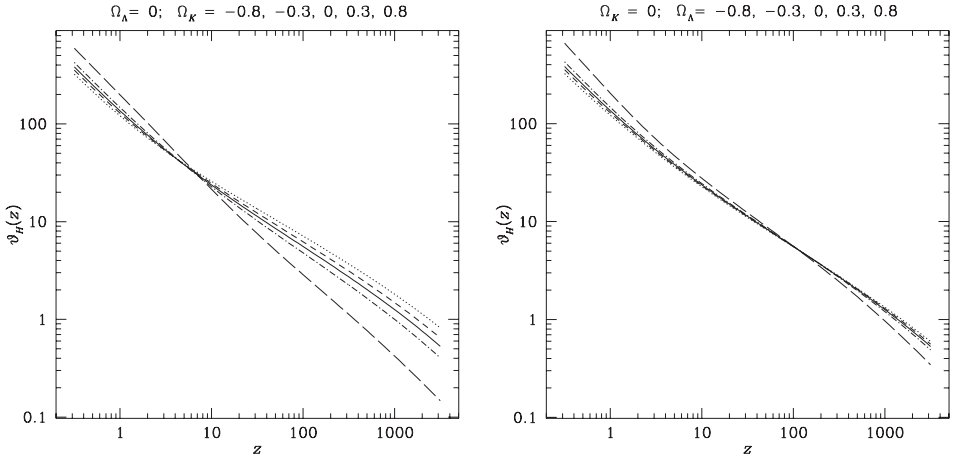


Fig. 1.4. $\vartheta_H(z_1)$ (in degrees) for different values of the cosmological parameters Ω_K and Ω_Λ the line styles are as in Fig. 1.3.

with Eq. (1.48) allows us, in principle, to determine the parameters Ω_m , Ω_Λ , Ω_K and H_0 .

Observationally we know for certain that $10^{-5} < \Omega_r \leq 10^{-4}$ as well as $0.1 \leq \Omega_m \lesssim 1$, $|\Omega_\Lambda| \lesssim 1$ and $|\Omega_K| \lesssim 1$.

If we are interested in small redshifts, $z_1 \lesssim 10$, we may therefore safely neglect Ω_r . In this region, Eq. (1.48) is very sensitive to Ω_Λ and provides an excellent mean to constrain the cosmological constant.

At high redshift, $z_1 \gtrsim 1000$, neglecting radiation is no longer a good approximation.

We shall later also need the opening angle of the *horizon* distance,

$$\vartheta_H(z_1) = \frac{t_1}{\chi(t_0 - t_1)}, \quad (1.49)$$

$$t_1 = \frac{1}{H_0 a_0} \int_{z_1}^{\infty} \frac{dz}{[\Omega_r(z+1)^4 + \Omega_m(z+1)^3 + \Omega_\Lambda + \Omega_K(z+1)^2]^{1/2}}. \quad (1.50)$$

(Clearly this integral diverges if $\Omega_r = \Omega_m = 0$. This is exactly what happens during an inflationary period and leads there to the solution of the horizon problem, see Section 1.5.)

Neglecting Ω_r , for $\Omega_\Lambda = 0$ and small curvature, $0 < |\Omega_K| < \Omega_m z_1$ at high enough redshift, $z_1 \geq 10$, one has $t_0 - t_1 \simeq 2\sqrt{|\Omega_K|/\Omega_m} = 2/(H_0 a_0 \sqrt{\Omega_m})$. With $\chi(x) \simeq x$, which is valid for small curvature, this yields $\vartheta(\Delta, z_1) \simeq \sqrt{\Omega_m} H_0 a_0 \Delta / (2a_1) = \frac{1}{2} \sqrt{\Omega_m} H_0 \Delta / (z_1 + 1)$ (see also Ex. 1.8).

Another important distance measure in cosmology is the luminosity distance. It is defined as follows. Let L be the luminosity (energy emitted per second) of a source at redshift z_1 and F its flux (energy received per second per square centimetre) arriving at the observer position. We define the luminosity distance to the source by

$$D_L(z_1) \equiv \left(\frac{L}{4\pi F} \right)^{1/2}. \quad (1.51)$$

We now want to show that $D_L(z_1) = (1 + z_1)^2 D_A(z_1)$.

In a proper time interval of the emitter, $d\tau_1 = a(t_1) dt$, the source emits the energy $La(t_1) dt$. This energy is redshifted by a factor of $(1 + z_1)^{-1} = a(t_1)/a(t_0)$. It is then distributed over a sphere with radius $a(t_0)\chi(t_0 - t_1)$. So that the flux per proper time of the observer $d\tau_0 = a(t_0) dt$ becomes

$$F = \frac{La^2(t_1)}{4\pi a^4(t_0)\chi^2(t_0 - t_1)},$$

leading to

$$D_L(z_1) = \frac{a(t_0)^2}{a(t_1)} \chi(t_0 - t_1) = (1 + z_1)^2 D_A(z_1). \quad (1.52)$$

The luminosity distance hence contains two additional factors $(1 + z)$ compared to the angular diameter distance. One of them is due to the ‘redshift’ of proper time and the other is due to the redshift of photon energy.

1.3 Recombination and decoupling

We assume that, at sufficiently early times, reaction rates for particle interactions are much faster than the expansion rate, so that the cosmic fluid is in thermal equilibrium. During its expansion, the Universe then cools adiabatically. At early times, it is dominated by a relativistic radiation background with

$$\rho = C/a^4 = g_{\text{eff}} a_{SB} T^4. \quad (1.53)$$

This behaviour implies that $T \propto a^{-1}$. Here g_{eff} is the effective number of degrees of freedom, which we define below and a_{SB} is the Stefan–Boltzmann constant, $a_{SB} = \pi^2/30$ in our units. For massless (or extremely relativistic) fermions and bosons in thermal equilibrium at temperature T with N_b respectively N_f spin degrees of freedom we have (remember that we use units such that $\hbar = k_B = c = 1$)

$$\begin{aligned} \rho_b &= \frac{N_b 4\pi}{(2\pi)^3} \int_0^\infty \frac{p^3 dp}{\exp(p/T) - 1} = \frac{N_b T^4}{2\pi^2} \int_0^\infty \frac{x^3 dx}{\exp(x) - 1} \\ &= \frac{N_b T^4}{2\pi^2} \Gamma(4)\zeta(4) = \frac{N_b T^4 \pi^2}{30}, \end{aligned} \quad (1.54)$$

$$\begin{aligned} \rho_f &= \frac{N_f 4\pi}{(2\pi)^3} \int_0^\infty \frac{p^3 dp}{\exp(p/T) + 1} = \frac{N_f T^4}{2\pi^2} \int_0^\infty \frac{x^3 dx}{\exp(x) + 1} \\ &= \frac{N_f T^4}{2\pi^2} \Gamma(4)\zeta(4) \frac{7}{8} = \frac{7}{8} \frac{N_f T^4 \pi^2}{30}, \end{aligned} \quad (1.55)$$

where Γ denotes the Gamma-function and ζ is the Riemann zeta-function and we make use of the integrals (Gradshteyn & Ryzhik, 2000)

$$I_b(\alpha) = \int_0^\infty \frac{x^\alpha dx}{\exp(x) - 1} = \Gamma(\alpha + 1)\zeta(\alpha + 1), \quad (1.56)$$

$$I_f(\alpha) = \int_0^\infty \frac{x^\alpha dx}{\exp(x) + 1} = \left[1 - \left(\frac{1}{2}\right)^\alpha \right] \Gamma(\alpha + 1)\zeta(\alpha + 1). \quad (1.57)$$

Furthermore, $\zeta(2) = \pi^2/6$, $\zeta(4) = \pi^4/90$, and $\Gamma(n) = (n - 1)!$ for $n \in \mathbb{N}$, see Abramowitz & Stegun (1970).

Hence $\rho = \rho_b + \rho_f = g_{\text{eff}} a_{SB} T^4$ for $a_{SB} = \pi^2 k_B^4 / (30 \hbar^3 c^2) = \pi^2/30$ and $g_{\text{eff}} = N_b + 7/8 N_f$, if all the particles are at the same temperature T . If the temperatures are different, like e.g., the neutrino temperature after electron–positron annihilation, this has to be taken into account with a factor $(T_\nu/T_\gamma)^4$.

At temperatures below the electron mass, $T < m_e \sim 0.5$ MeV only neutrinos and photons are still relativistic. Very recently, $T \lesssim 0.01$ eV the neutrinos also become non-relativistic so that the density parameter of relativistic particles today

is given only by the photon density,

$$\Omega_{\text{rel}} = \Omega_\gamma = \frac{16\pi G}{3H_0^2} a_{SB} T_0^4 = 2.49 \times 10^{-5} h^{-2}. \quad (1.58)$$

Here we have set $T_0 = 2.725$ K (see [Particle Data Group, 2006](#)).

The pressure of relativistic particles is given by $P = T_i^i/3 = \rho/3$. The thermodynamic relation $dE = T dS - P dV$ therefore gives for entropy density $s = dS/dV$

$$s = \frac{dS}{dV} = \frac{1}{T} \left(\frac{dE}{dV} + P \right) = \frac{\rho + P}{T} = \frac{4\rho}{3T}. \quad (1.59)$$

Using the expression for the energy density (1.54) and (1.55) this gives for each particle species X

$$s_X = \begin{cases} \frac{2\pi^2}{45} N_X T^3 & \text{for bosons,} \\ \frac{7\pi^2}{180} N_X T^3 & \text{for fermions.} \end{cases} \quad (1.60)$$

The particle density for relativistic particles is given by

$$n_X = \frac{N_X}{2\pi^2} \int \frac{p^2}{\exp(p/T) \pm 1} dp = \begin{cases} T^3 \frac{N_X}{\pi^2} \zeta(3) & \text{for bosons,} \\ T^3 \frac{N_X}{\pi^2} \zeta(3) \frac{3}{4} & \text{for fermions.} \end{cases} \quad (1.61)$$

The particle and entropy densities both scale like T^3 . Using $\zeta(3) \simeq 1.202\,057$ we obtain

$$s_X \simeq \begin{cases} 3.6 \cdot n_X & \text{for bosons,} \\ 4.2 \cdot n_X & \text{for fermions.} \end{cases} \quad (1.62)$$

The photons obey a Planck distribution ($\epsilon = ap =$ the photon energy),

$$f(\epsilon) = \frac{1}{e^{\epsilon/T} - 1}. \quad (1.63)$$

At a temperature of about $T \sim 4000$ K ~ 0.4 eV, the number density of photons with energies above the hydrogen ionization energy ($= \Delta = 1$ Ry $= 13.6$ eV) drops below the baryon density of the Universe, and the protons begin to (re)combine to neutral hydrogen. (Helium has already recombined earlier.) Photons and baryons are tightly coupled before (re)combination by Thomson scattering of electrons. During recombination the free electron density drops sharply and the mean free path of the photons grows larger than the Hubble scale. At the temperature $T_{\text{dec}} \sim 3000$ K (corresponding to the redshift $z_{\text{dec}} \simeq 1100$ and the physical time $t_{\text{dec}} \simeq a_{\text{dec}} \eta_{\text{dec}} \simeq 10^5$ yr) photons decouple from the electrons and the Universe becomes transparent. We now want to study this process in somewhat more detail.

1.3.1 The physics of recombination

As we have seen above, the photon entropy is given by

$$s_\gamma = \frac{4\pi^2}{45} T^3 \simeq 3.6 n_\gamma.$$

The conserved baryon number n_B satisfies $a^3 n_B = \text{constant}$, hence $n_B \propto a^{-3} \propto T^3$. The entropy per baryon is therefore a constant,

$$\sigma = s_\gamma/n_B = \frac{\frac{4\pi^2}{45} T_0^3}{\Omega_B \rho_c(\tau_0)/m_p} = 1.4 \times 10^8 \frac{T_{2.7}^3}{\Omega_B h^2}. \quad (1.64)$$

Here we have used (see Appendix 1)

$$\begin{aligned} \rho_c(\tau_0) &= 1.88 h^2 \times 10^{-29} \text{ g cm}^{-3} = 8.1 h^2 \times 10^{-11} (\text{eV})^4, \\ m_p &= 9.38 \times 10^8 \text{ eV}, \quad (\text{proton mass}), \\ T(\tau_0) &= 2.3 T_{2.7} \times 10^{-4} \text{ eV}, \quad T_{2.7} = T(\tau_0)/2.7 \text{ K}. \end{aligned}$$

As we shall see in the next section, the baryon density is approximately $\Omega_B h^2 \simeq 2 \times 10^{-2}$ so that $\sigma \simeq 10^{10}$. Correspondingly the ratio between photon and baryon density is

$$\eta_B = n_B/n_\gamma = 2.7 \times 10^{-8} \left(\frac{\Omega_B h^2}{T_{2.7}^3} \right). \quad (1.65)$$

As long as hydrogen is ionized, the timescale of interaction between photons and electrons (Thomson scattering) and between electrons and protons (Rutherford scattering) is much faster than expansion and we may therefore consider the latter as adiabatic. At every moment, the electron, proton, photon plasma is in thermal equilibrium. As long as the temperature is above the ionization energy of neutral hydrogen, $T > 1 \text{ Ry} = \Delta = \alpha^2 m_e/2 = 13.6 \text{ eV}$ all hydrogen atoms that form are rapidly dissociated. Most electrons and protons are free and the neutral hydrogen density is very low. At some sufficiently low temperature, however, there will no longer be sufficiently many energetic photons around to disrupt neutral hydrogen and the latter becomes more and more abundant. To determine the temperature at which this transition, called ‘recombination’,³ happens, we apply the standard rules of equilibrium statistical mechanics to the reaction



Supposing that pressure and temperature are fixed and only the number of free electrons, N_e , free protons, N_p , hydrogen atoms, N_H , and photons, N_γ , can change,

³ The expression ‘combination’ would be more adequate, since this is the first time that neutral hydrogen forms, but it is difficult to change historical mis-namings. . . .

the second law of thermodynamics implies that the Gibbs potential G is constant,

$$0 = dG = \mu_p dN_p + \mu_e dN_e + \mu_H dN_H + \mu_\gamma dN_\gamma ,$$

Here μ_X denotes the chemical potential of species X . The different dN_X are not independent. Particle number conservation implies

$$dN_p + dN_H = dN_e + dN_\gamma = 0 . \quad (1.67)$$

As there is no conservation of photons, the chemical potential of photons is thus $\mu_\gamma = 0$. With this and Eq. (1.67) the Gibbs equation, $dG = 0$ implies

$$\mu_e + \mu_p - \mu_H = 0 . \quad (1.68)$$

In this discussion, where we are more interested in the basic concepts than in accuracy we neglect helium which has recombined earlier. We shall set $n_p + n_H = n_B$ which induces an error of about 25%. For an accurate calculation of the final ionization fraction, one would have to take into account both, the recombination of helium and the recombination into excited states of hydrogen. It is actually interesting to note that recombination into the ground state (1S) is not efficient at all since the ionization cross section is very high for resonant Ly α photons so that most of these just ionize another hydrogen atom leading to no net recombination. The same is true for recombination into the 2P excited state. It is more efficient if electrons are captured into the 2S level from which they can decay into the ground state via the emission of two photons. By angular momentum conservation, the emission of a single photon is not possible. The inverse process, excitation from 1S to 2S is a three-body process and therefore highly unlikely. Even though the rate of the transition $(e, p) \rightarrow \text{H}_{2\text{S}} \rightarrow \text{H}_{1\text{S}}$ is relatively low, it wins against direct recombination into the ground state and subsequent cosmological redshifting of the photon before the next ionization can take place. More details are found in [Peebles \(1993\)](#), [Mukhanov \(2005\)](#), [Rubino-Martin *et al.* \(2006\)](#) and [Wong *et al.* \(2006\)](#). Despite this fact, a discussion of recombination into the ground state captures the main features of the process and the correct recombination and decoupling redshifts do not significantly differ from those obtained here.

In thermal equilibrium, electrons, protons and hydrogen atoms obey a Maxwell–Boltzmann distribution. Their number densities are given by (see Ex. 1.5)

$$n_e = \frac{2}{(2\pi)^3} (2\pi m_e T)^{3/2} \exp\left(-\frac{m_e - \mu_e}{T}\right), \quad (1.69)$$

$$n_p = \frac{2}{(2\pi)^3} (2\pi m_p T)^{3/2} \exp\left(-\frac{m_p - \mu_p}{T}\right), \quad (1.70)$$

$$n_H = \frac{4}{(2\pi)^3} (2\pi m_H T)^{3/2} \exp\left(-\frac{m_H - \mu_H}{T}\right). \quad (1.71)$$

We now make use of the fact that the Universe is globally neutral, $n_e = n_p$. Furthermore, the binding energy of hydrogen $\Delta = \alpha^2 m_e / 2$ (here $\alpha \simeq 1/137$ is the fine structure constant) is given by $\Delta = m_e + m_p - m_H$. With this we obtain

$$\frac{n_e^2}{n_H} = \frac{n_e n_p}{n_H} = \left(\frac{m_e T}{2\pi} \right)^{3/2} e^{-\Delta/T}. \quad (1.72)$$

Here we have neglected the small difference between the hydrogen and the proton mass in the second factor of Eqs. (1.70) and (1.71) but not in the exponential.

We now define the ionization fraction x_e by $x_e \equiv n_e / (n_e + n_H)$. Eq. (1.72) then leads to

$$\frac{x_e^2}{1 - x_e} = \frac{n_e^2}{n_H(n_p + n_H)} = \frac{1}{n_B} \left(\frac{m_e T}{2\pi} \right)^{3/2} e^{-\Delta/T}. \quad (1.73)$$

Inserting the entropy per baryon, $\sigma = (4\pi^2/45)T^3/n_B$, in this equation yields

$$\frac{x_e^2}{1 - x_e} = \frac{45\sigma}{4\pi^2} \left(\frac{m_e}{2\pi T} \right)^{3/2} e^{-\Delta/T}. \quad (1.74)$$

This is the *Saha equation*. At very high temperatures, $T \gg \Delta$, the ionization fraction x_e is close to 1. Recombination happens roughly when $\sigma \exp(-\Delta/T)$ is of the order of unity. If $\sigma \sim 1$ this corresponds to $T \sim \Delta$. The fact that the entropy per baryon is very large, $\sigma = 1.4 \times 10^8 (\Omega_B h^2)^{-1} \sim 10^{+10}$ delays recombination significantly. Since there are so many more photons than baryons in the Universe, even at a temperature much below $\Delta = 13.6$ eV there are still enough photons in the high-temperature tail of the Planck distribution to keep the Universe ionized.

To be more specific we define the recombination temperature T_{rec} as the temperature when $x_e = 0.5$ (as we shall see, the precise value is of little importance). Eq. (1.74) then leads to

$$\left(\frac{T_{\text{rec}}}{1 \text{ eV}} \right)^{-3/2} e^{-\Delta/T_{\text{rec}}} = 1.3 \times 10^{-16} \Omega_B h^2. \quad (1.75)$$

For $\Omega_B h^2 \simeq 0.02$ we obtain

$$T_{\text{rec}} = 3757 \text{ K} = 0.32 \text{ eV}, \quad z_{\text{rec}} = 1376.$$

The function $x_e(T)$ is shown in Fig. 1.5. Clearly, this function grows very steeply from $x_e \sim 0$ to $x_e \sim 1$ at $T \sim 3700$ K and T_{rec} depends only weakly on the value chosen for $x_e(T_{\text{rec}})$.

Interestingly, at temperature T_{rec} the baryon and photon densities are of the same order, $\rho_\gamma(T_{\text{rec}}) \simeq \rho_B(T_{\text{rec}})$. This seems to be a complete coincidence. More

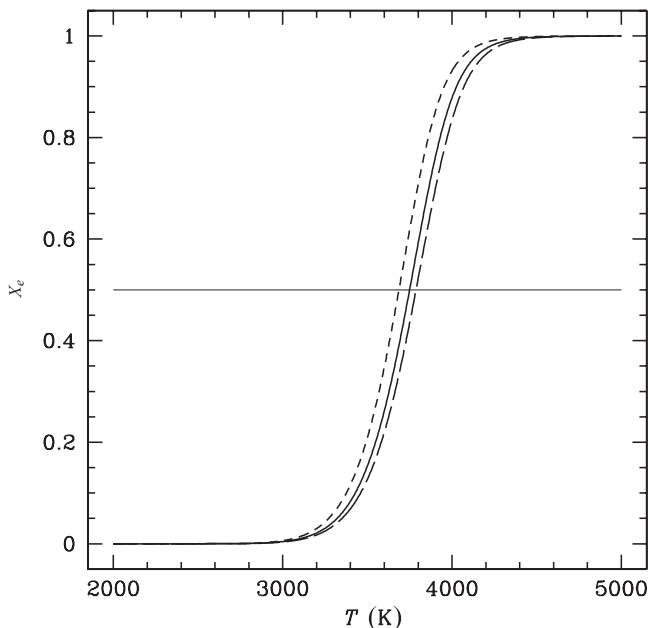


Fig. 1.5. The ionization fraction x_e as a function of the temperature is obtained via the Saha equation for $\Omega_B h^2 = 0.02$ (solid curve), for $\Omega_B h^2 = 0.03$ (long-dashed curve) and for $\Omega_B h^2 = 0.01$ (short-dashed curve). Our definition of recombination, $x_{\text{rec}} = 0.5$, is indicated. Note that x decays from $x_e \simeq 1$ to $\simeq 0$ between $T = 4000$ and 3400 K.

precisely, the ratio of these two densities is given by

$$\begin{aligned} \frac{\rho_\gamma}{\rho_B} &= \frac{(\pi^2/15)T^4}{n_B m_p} = \frac{\pi^2 T_0^4}{15 n_B(t_0) m_p} (z+1) \\ &\simeq 2 \times 10^{-5} (\Omega_B h^2)^{-1} (z+1). \end{aligned} \quad (1.76)$$

This ratio is equal to 1 at redshift z_{rb} given by

$$(1 + z_{rb}) = 10^3 \left(\frac{\Omega_B h^2}{2 \times 10^{-2}} \right) \simeq 10^3 \sim 1 + z_{\text{rec}}. \quad (1.77)$$

1.3.2 Final ionization and photon decoupling

We have determined the temperature at which electrons and protons recombine to neutral hydrogen. As the free electron fraction drops, the interaction rate between electrons and protons decreases and at some point, the remaining free electrons and protons are too sparse to find each other, so that the number of free electrons remains constant. But also the photon–electron interaction rate decreases. Whenever

an interaction rate Γ drops below the expansion rate of the Universe,

$$\Gamma < H ,$$

one considers the corresponding reaction as ‘frozen’. It becomes negligible. When the recombination rate drops below the expansion rate, recombination freezes and the ionization fraction remains constant. When the scattering rate of photons on electrons falls below the expansion rate of the Universe, photons become free to propagate without further scattering. We want to calculate both, the final ionization, x_R , and the redshift z_{dec} of the decoupling of photons. Let us first determine the temperature T_g at which the process of reionization freezes out. The cross section of the reaction $p^+ + e^- \rightarrow \text{H} + \gamma$ is (see, e.g. [Rybicki & Lightman, 1979](#))

$$\langle \sigma_{Rv} \rangle \simeq 4.7 \times 10^{-24} \left(\frac{T}{1 \text{ eV}} \right)^{-1/2} \text{ cm}^2 . \quad (1.78)$$

Here v is the thermal electron velocity and we have used the fact that $3T = m_e v^2$. The reaction rate is therefore

$$\begin{aligned} \Gamma_R &= n_p \langle \sigma_{Rv} \rangle = x_e \left(\frac{n_B}{n_\gamma} \right) n_\gamma \langle \sigma_{Rv} \rangle \\ &\simeq 2.4 \times 10^{-10} \text{ cm}^{-1} \left(\frac{T}{1 \text{ eV}} \right)^{7/4} \exp(-\Delta/2T) (\Omega_B h^2)^{1/2} , \end{aligned}$$

where we have inserted the Saha equation, assuming that the ionization fraction is much smaller than 1, i.e.,

$$x_e \simeq (\sqrt{45} \sigma / 2\pi) (m_e / 2\pi T)^{3/4} \exp(-\Delta/2T) \ll 1 .$$

We have also used Eq. (1.65).

To determine the expansion rate $H(T)$, we neglect curvature or a possible cosmological constant, which is certainly a good approximation for all redshifts larger than, say, 5. We also assume that the Universe is matter dominated at freeze-out, which induces an error of about 15% in H . The Friedmann equation (1.18) then gives

$$\begin{aligned} H^2 &\simeq \frac{8\pi G}{3} \rho \simeq \frac{8\pi G}{3} \rho_0 (a_0/a)^3 \\ &= \frac{8\pi G}{3} \Omega_m \rho_c(t_0) (T/T_0)^3 , \end{aligned}$$

so that

$$H \simeq 3 \times 10^{-23} \text{ cm}^{-1} (\Omega_m h^2)^{1/2} \left(\frac{T}{1 \text{ eV}} \right)^{3/2} . \quad (1.79)$$

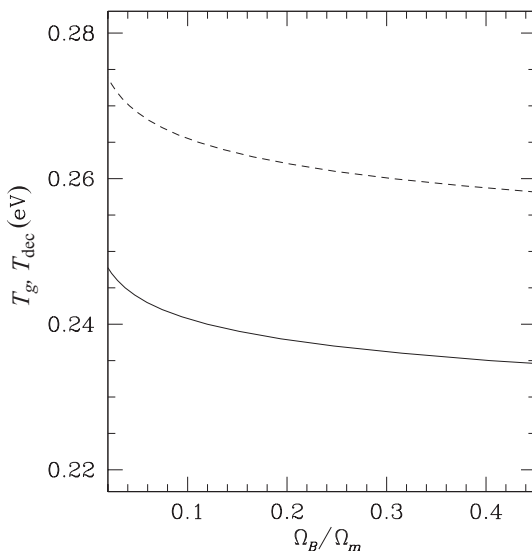


Fig. 1.6. The freeze-out temperatures of recombination (solid curve) and of Thomson scattering (dashed curve) as functions of Ω_B/Ω_m .

Eq. (1.79) is a very useful formula, valid whenever the Universe is dominated by non-relativistic matter, dust, $P \ll \rho$, and curvature or a cosmological constant are negligible.

The temperature T_g is defined by $\Gamma_R(T_g) = H(T_g)$, which finally leads to

$$\left(\frac{T_g}{1 \text{ eV}}\right)^{1/4} e^{-\Delta/2T_g} = 1.2 \times 10^{-13} \left(\frac{\Omega_m}{\Omega_B}\right)^{1/2}. \quad (1.80)$$

This result is independent of h . For $\Omega_m \simeq 7\Omega_B$ (the value inferred from observations (Spergel *et al.*, 2003)), we obtain $T_g \simeq 0.24 \text{ eV}$ and $z_g \simeq 1010$ (see Fig. 1.6). T_g depends only weakly on the ratio Ω_B/Ω_m .

The final ionization fraction is given by

$$x_R \simeq x_e(T_g) \simeq 7.3 \times 10^{-6} \left(\frac{T_g}{1 \text{ eV}}\right)^{-1} \Omega_m^{1/2}/(\Omega_B h) \simeq 3 \times 10^{-5} \Omega_m^{1/2}/(\Omega_B h). \quad (1.81)$$

A more detailed numerical analysis, taking into account the contribution from radiation to the expansion rate and the recombination into excited states of the hydrogen atoms and the presence of helium (see next section) gives $x_R \sim 1.2 \times 10^{-5} \Omega_m^{1/2}/(\Omega_B h)$ (Peebles, 1993; Mukhanov, 2005). We can use this result to calculate the optical depth τ to Thomson scattering of photons by free electrons up to a redshift $z < z_g$ in a recombined universe. The optical depth to z is the scattering probability of a photon integrated from z until today. With the Thomson

cross section

$$\sigma_T = \frac{8\pi}{3}\alpha^2 m_e^{-2} \simeq 6.65 \times 10^{-25} \text{ cm}^2, \quad (1.82)$$

one finds

$$\tau(z) \equiv \int_{t(z)}^{t_0} \sigma_T n_e \frac{dt}{a} \simeq 0.046 x_R (1+z)^{3/2} \Omega_B \Omega_m^{-1/2} h. \quad (1.83)$$

With the residual ionization above we find $\tau(z=800) \simeq 0.01$. As we shall see in Section 6.3 the Universe is reionized at low redshift $z \sim 10$, which increases the optical depth by roughly a factor of 10. This rescattering of CMB photons is relevant for the evolution of fluctuations as we shall discuss in Section 6.3.

As long as the temperature is larger than T_g , the reaction $p + e \longleftrightarrow \text{H} + \gamma$ is in thermal equilibrium. When the temperature drops below T_g , the recombination process freezes out and the degree of ionization remains nearly constant.

Let us also note that in deriving the Saha equation (1.74), we used the fact that the process of recombination is in thermal equilibrium, which we have verified only now since freeze-out happens after recombination, $T_g < T_{\text{rec}}$.

We finally calculate the redshift of the decoupling of photons. The process which remains effective longest is elastic Thomson scattering. Its rate is given by

$$\begin{aligned} \Gamma_T &= \sigma_T n_e = \sigma_T x_e \left(\frac{n_B}{n_\gamma} \right) n_\gamma \\ &\simeq 3.4 \times 10^{-11} \text{ cm}^{-1} (\Omega_B h^2)^{1/2} \left(\frac{T}{1 \text{ eV}} \right)^{9/4} \exp(-\Delta/2T). \end{aligned} \quad (1.84)$$

Comparing it to the expansion rate, we find T_{dec} which is defined by $H(T_{\text{dec}}) = \Gamma_T(T_{\text{dec}})$. A rough estimate gives $T_{\text{dec}} \sim 0.26 \text{ eV}$ (see Fig. 1.6) which corresponds to $z_{\text{dec}} \sim 1100$. Again we have assumed $x_e \ll 1$ in Eq. (1.84) which is justified since $T_{\text{dec}} \sim 3000 \text{ K}$ (see Fig. 1.5).

Even though after z_{dec} photons decouple from electrons, the latter are still coupled to photons. The scattering rate of electrons, given by $\Gamma_e = \sigma_T x_e n_\gamma \gg \sigma_T n_e$, is sufficient to keep the electrons and with them the matter in thermal equilibrium with the photons until very low redshift. Therefore, even after recombination the matter temperature is equal to the temperature of the CMB and does not decay like $1/a^2$ as would be expected from a pure thermal gas of massive particles (see page 25).

1.3.3 Propagation of free photons and the CMB

After t_{dec} , photons cease any interaction with the cosmic fluid and propagate freely. It is straight forward to estimate that the cross section for Rayleigh scattering with hydrogen atoms is much too weak to be relevant.

The free propagation of photons after decoupling is described with the Liouville equation for the photon distribution function, which we now develop. Since photons do not interact anymore, they simply move along geodesics. The Liouville equation translates this to a differential equation for the 1-particle distribution function f of the photons. The function f describes the particle density in the phase space P_0 , the photon mass-shell, given by

$$P_0 = \{(x, p) \in T\mathcal{M} \mid g_{\mu\nu}(x)p^\mu p^\nu = 0\}, \quad f : P_0 \rightarrow \mathbb{R}.$$

The distribution function f gives the number of particles per phase space volume $|g| d^3x d^3p$ at fixed time t . In some general geometry a specific space-like hypersurface Σ has to be chosen and one then has to show that f does not depend on this choice (more details are found in Ehlers (1971) and Stewart (1971)). In cosmology, due to the symmetries present, we simply use the hypersurfaces of constant time, $\Sigma = \Sigma_t$.

We choose the coordinates (x^μ, p^i) on the seven-dimensional mass-shell ($0 \leq \mu \leq 3$ and $1 \leq i \leq 3$). The energy p^0 is then determined by the mass-shell condition $g_{\mu\nu}(x)p^\mu p^\nu = 0$. Liouville's equation now says that the 1-particle distribution remains unchanged if we follow the geodesic motion of the particles, i.e.,

$$\begin{aligned} 0 &= \frac{df}{dt} = \dot{x}^\mu \partial_\mu f + \dot{p}^i \frac{\partial f}{\partial p^i}, \\ 0 &= p^\mu \partial_\mu f - \Gamma_{\mu\nu}^i p^\mu p^\nu \frac{\partial f}{\partial p^i} \equiv L_{X_g} f. \end{aligned} \quad (1.85)$$

A particle distribution obeying this equation is often also called a geodesic spray (see Abraham & Marsden, 1982). If the particles are not free, but collisions are so rare that an equilibrium description is not adequate, one uses the Boltzmann equation,

$$L_{X_g} f = C[f], \quad (1.86)$$

where $C[f]$ is the so-called 'collision integral' which depends on the details of the interactions.

It may be disturbing to some readers that we take over these concepts from non-relativistic physics so smoothly to the relativistic case. In cosmology, this does not cause any problems. But in general, it is true that the collision integral is not always

well defined and certain conditions have to be posed to the nature of the spacetime and of the interaction. This problem has been studied in detail by Ehlers (1971).

Since the photons are massless, $|\mathbf{p}|^2 = \gamma_{ij} p^i p^j = (p^0)^2$. Here p^0 is the 0-component of the momentum 4-vector in *conformal* time so that $\epsilon = ap^0$ is the physical photon energy. Isotropy of the distribution implies that f depends on p^i only via $p \equiv |\mathbf{p}| = p^0$, and so

$$\frac{\partial f}{\partial p^i} = \frac{\partial p}{\partial p^i} \frac{\partial f}{\partial p} = \frac{p_i}{p} \frac{\partial f}{\partial p}. \quad (1.87)$$

Furthermore, f depends on x^i only through $p = \sqrt{\gamma_{ij} p^i p^j}$. Spatial derivatives are therefore given by

$$\begin{aligned} p^i \partial_i f &= p^i \gamma_{lm,i} \frac{p^l p^m}{p} \frac{\partial f}{\partial p} = p_j \gamma^{ij} \gamma_{lm,i} \frac{p^l p^m}{p} \frac{\partial f}{\partial p} \\ &= \frac{1}{2} \gamma^{ij} (\gamma_{li,m} + \gamma_{mi,l} - \gamma_{lm,i}) \frac{p_j p^l p^m}{p} \frac{\partial f}{\partial p} \\ &= \Gamma_{lm}^j \frac{p^l p^m p_j}{p} \frac{\partial f}{\partial p}. \end{aligned}$$

This leads to

$$p^i \partial_i f - \Gamma_{\mu\nu}^i \frac{p^\mu p^\nu p_i}{p} \frac{\partial f}{\partial p} = -(\Gamma_{j0}^i + \Gamma_{0j}^i) \frac{p^j p p_i}{p} \frac{\partial f}{\partial p} = -2p^2 \frac{\dot{a}}{a} \frac{\partial f}{\partial p},$$

where we have used the expressions in Appendix A2.3 for $\Gamma_{\mu\nu}^i$ and $p = p^0$. Inserting this result into (1.85) we obtain, with Eq. (1.87),

$$\partial_t f - 2p \frac{\dot{a}}{a} \frac{\partial f}{\partial p} = 0, \quad (1.88)$$

which is satisfied by an arbitrary function $f = f(pa^2) = f(a\epsilon)$. Hence the distribution of free-streaming photons changes only by redshifting the *physical energy* $\epsilon = ap^0$ or the *physical momentum* $a|\mathbf{p}| = \epsilon$. Therefore, setting $T \propto a^{-1}$ even after recombination, the blackbody shape of the photon distribution remains unchanged. This radiation of free photons with a perfect blackbody spectrum is the CMB. Its physics, especially its fluctuation and polarization are the main topic of this book.

The same result is also obtained for massive particles,

$$\partial_t f - 2p \frac{\dot{a}}{a} \frac{\partial f}{\partial p} = 0, \quad (1.89)$$

where $p = |\mathbf{p}|$; hence the momentum is simply redshifted. Therefore, massive particles which decouple when they are still relativistic, keep their extremely relativistic Fermi–Dirac (or Bose–Einstein) distribution, $f = (\exp(ap/T) \pm 1)$, with a

temperature which simply scales as $T \propto 1/a$. This is especially important for the cosmic neutrinos which probably have masses in the range of a few $\text{eV} > m_\nu \gtrsim 0.01 \text{ eV}$. But, as we shall see in the next section, they decouple at $T \sim 1.4 \text{ MeV}$. We therefore expect them to be distributed according to an extremely relativistic Fermi–Dirac distribution.

Note however, that after decoupling the particles are no longer in thermal equilibrium and the T in their distribution function is not a temperature in the thermodynamical sense but merely a parameter, representing a measure of the mean kinetic energy.

The situation is different for the electron–proton–hydrogen plasma. The free electrons still scatter with photons and keep the same temperature as the latter. In other words: even though most photons are no longer interacting with the electrons, the latter are still interacting with the photons. (To have one collision with all the remaining electrons, only a fraction of about 10^{-14} of the photons have to be involved!)

Soon after recombination, the baryon energy density exceeds the photon energy density and one might expect that this would change the evolution of the temperature. To investigate this we use the energy conservation equation of the baryon–photon system. We neglect the tiny number of free electrons. The energy density and pressure are then given by

$$\rho = n_B m_B + (3/2)n_B T + \frac{\pi^2}{15} T^4, \quad (1.90)$$

$$p = n_B T + \frac{\pi^2}{45} T^4. \quad (1.91)$$

The energy conservation equation, $d\rho/da = -3(\rho + p)/a$ now gives

$$\frac{a}{T} \frac{dT}{da} = -\frac{3n_B + \frac{4\pi^2}{15} T^3}{(3/2)n_B + \frac{4\pi^2}{15} T^3} = -\frac{\sigma + 1}{\sigma + 1/2}. \quad (1.92)$$

Since $\sigma \gg 1$, the photons are so much more numerous than the baryons that the latter have no influence on the temperature which keeps evolving as $1/a$. Note, however, that in the absence of photons, the temperature of a mono-atomic gas would decrease like $1/a^2$ (just consider the limit $\sigma \rightarrow 0$).

The blackbody spectrum of the CMB photons is extremely well verified observationally (see Fig. 1.7 and Chapter 8). The limits on deviations are often parametrized in terms of three parameters: the chemical potential μ , the Compton- y parameter (which quantifies a well defined change in the spectrum arising from interactions with a non-relativistic electron gas at a different temperature, see Chapter 8) and Y_{ff} (describing a contamination by free–free emission).

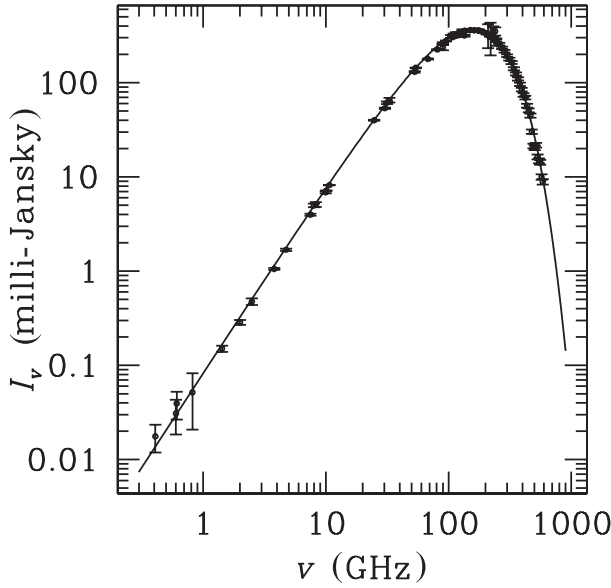


Fig. 1.7. The spectrum of the cosmic background radiation. The data are from many different measurements which are all compiled in [Kogut *et al.* \(2006\)](#). The points around the top are the measurements from the FIRAS experiment on COBE ([Fixsen *et al.*, 1996](#)). The line traces a blackbody spectrum at a temperature of 2.728 K (the data are courtesy of Susan Staggs).

The present 95% confidence limits on these parameters are ([Particle Data Group, 2006](#))

$$|\mu| < 9 \times 10^{-5}, \quad |y| < 1.2 \times 10^{-5}, \quad |Y_{\text{ff}}| < 1.9 \times 10^{-5}. \quad (1.93)$$

The CMB photons not only have a very thermal spectrum, but they are also distributed very isotropically, apart from a dipole which is (most probably) mainly due to our motion relative to the surface of last scattering.

Indeed, an observer moving with velocity \mathbf{v} relative to a source in direction \mathbf{n} emitting a photon with proper momentum $\mathbf{p} = -\epsilon\mathbf{n}$ sees this photon redshifted with frequency

$$\epsilon' = \gamma\epsilon(1 - \mathbf{nv}), \quad (1.94)$$

where $\gamma = 1/\sqrt{1 - v^2}$ is the relativistic γ -factor. For an isotropic emission of photons coming from all directions \mathbf{n} this leads to a dipole anisotropy to first order in \mathbf{v} . This dipole anisotropy, which is of the order of

$$\left(\frac{\Delta T}{T}\right)_{\text{dipole}} \simeq 1.2 \times 10^{-3},$$

has already been discovered in the seventies (Conklin, 1969; Henry, 1971). Interpreting it as due to our motion with respect to the last scattering surface implies a velocity for the solar system barycentre of $v = 371 \pm 0.5 \text{ km s}^{-1}$ at 68% CL (Particle Data Group, 2006).

In addition to the dipole, the COBE⁴ DMR experiment (differential microwave radiometer) has found fluctuations of order

$$\sqrt{\left\langle \left(\frac{\Delta T}{T} \right)^2 \right\rangle} \sim (\text{a few}) \times 10^{-5}, \quad (1.95)$$

on all angular scales $\theta \geq 7^\circ$ (Smoot *et al.*, 1992). On smaller angular scales many experiments found fluctuations (we shall describe the experimental results in more detail later), but all of them satisfy $|\Delta T/T| \lesssim 10^{-4}$.

As we shall see in Chapter 2, the CMB fluctuations on large scales provide a measure for the deviation of the geometry from the Friedmann–Lemaître one. The geometry perturbations are thus small, and we may calculate their effects by *linear perturbation theory*. On smaller scales, $\Delta T/T$ reflects the fluctuations in the energy density in the baryon/radiation plasma prior to recombination. Their amplitude is just about right to allow the formation of the presently observed non-linear structures (like galaxies, clusters, etc.) by gravitational instability.

These findings strongly support our hypothesis that the large-scale structure (i.e., the galaxy distribution) observed in the Universe has been formed by gravitational instability from small ($\sim 10^{-4}$) initial fluctuations. As we shall see in Chapters 2, 4 and 5, such initial fluctuations leave an interesting ‘fingerprint’ on the cosmic microwave background.

1.4 Nucleosynthesis

1.4.1 Expansion dynamics at $T \sim \text{a few MeV}$

At high temperatures, $T > 30 \text{ MeV}$, none of the light nuclei (deuterium, ^2H , helium-4, ^4He , helium-3, ^3He or lithium, ^7Li) are stable. At these temperatures, we expect the baryons to form a simple mixture of protons and neutrons in thermal equilibrium with each other and with electrons, photons and neutrinos. The highest binding energy is the one of ^4He which is about 28 MeV. Nevertheless, ^4He cannot form at this temperature since the baryon density of the Universe is not high enough for three- or even four-body interactions to occur in thermal equilibrium. Therefore, before any nucleosynthesis can occur, the temperature has to drop below the binding energy of deuterium which is about 2.2 MeV. But even at this temperature there

⁴ Cosmic Background Explorer, NASA satellite launched 1990.

are still far too many high-energy photons around for deuterium to be stable. This is due to the very low baryon to photon ratio $\eta_B \simeq 10^{-10}$. Just as recombination is delayed from the naively expected temperature $T = 13.7$ eV to about $T_{\text{rec}} \sim 0.3$ eV, nucleosynthesis does not happen at $T \sim 2.2$ MeV but around $T_{\text{nuc}} \sim 0.1$ MeV. Most of the neutrons present at that temperature are converted into ${}^4\text{He}$. Only small traces remain as deuterium or are burned into ${}^3\text{He}$ and ${}^7\text{Li}$.

Let us study this in some more detail. At the time of recombination, the relativistic particle species are the photon and, probably three types of neutrinos. As we shall see in the next paragraph, the neutrino temperature is actually a factor of $(4/11)^{1/3}$ lower than the temperature of the photons. With Eqs. (1.54) and (1.55), the energy density of these particles while they are relativistic is given by

$$\rho_{\text{rel}}(t) = [\rho_\gamma(t) + \rho_\nu(t)] = \left[1 + 3\frac{7}{8}(4/11)^{4/3} \right] \frac{\pi^2}{15} T^4, \quad (1.96)$$

$$\simeq 10^{-33} \text{ g cm}^{-3} \left(\frac{T}{T_0} \right)^4, \quad (1.97)$$

$$\simeq \rho_c(t_0) \Omega_{\text{rel}} h^2 (1+z)^4, \text{ where} \\ \Omega_{\text{rel}} h^2 \simeq 4.4 \times 10^{-5}. \quad (1.98)$$

Note that at temperatures below the highest neutrino mass, this is no longer the energy density of relativistic particles, therefore Ω_{rel} is not the density parameter of relativistic particles today. Above the neutrino mass threshold and below the electron mass threshold we have

$$\frac{\rho_{\text{rel}}}{\rho_m} = \frac{\Omega_{\text{rel}}}{\Omega_m} (1+z) \simeq 4.4 \times 10^{-5} \left(\frac{1}{\Omega_m h^2} \right) (1+z), \quad (1.99)$$

Since $\Omega_m h^2 \simeq 0.15$, the redshift z_{eq} above which the Universe is dominated by relativistic particles is about

$$z_{\text{eq}} \simeq 3.4 \times 10^3, \quad T_{\text{eq}} \simeq 1 \text{ eV}. \quad (1.100)$$

At temperatures significantly above T_{eq} , we can also neglect a possible contribution from curvature or a cosmological constant to the expansion of the Universe, so that for

$$z \gg z_{\text{eq}} \quad P = \frac{1}{3} \rho, \quad a \propto \tau^{1/2} \propto t. \quad (1.101)$$

At these high temperatures the energy density of the Universe is given by

$$\rho = g_{\text{eff}} \frac{\pi^2}{30} T^4 \quad \text{where} \quad g_{\text{eff}} = N_B(T) + \frac{7}{8} N_F(T). \quad (1.102)$$